7.1 ION IRRADIATION EFFECTS ON HIGH ENTROPY ALLOY

— N. A. P. Kiran Kumar[1,2*], K. J. Leonard [1], H. Bei[1], T. S. Byun[1], Y. Zhang[1,2], and S. J. Zinkle[1] *(Oak Ridge National Laboratory[1], University of Tennessee[2])*

OBJECTIVE

The goal of this study is to investigate the basic radiation behavior of structurally unique High Entropy Alloy (HEA).

SUMMARY

Preliminary microstructural and nanoindentation examinations have been performed on Fe-28%Ni-27%Mn-18%Cr high entropy alloy specimens irradiated with 3 MeV Ni ions at room temperature to 0.1 and 1 dpa and at 500°C to 1 and 10 dpa. The hardness in the ion irradiated region of the crystalline face centered cubic HEA samples increased rapidly with increasing dose at room temperature, from ~40% higher than the unirradiated value at 0.1 dpa to approximately double the unirradiated hardness at 1 dpa. The increase in the irradiated hardness was less pronounced for irradiations at 500°C, with values of 15-20% increase at 1 dpa and ~20% increase at 10 dpa. Microstructural characterization of the irradiated HEA specimens found small defect clusters after room temperature irradiation and larger defect clusters after 500°C irradiation; voids were not observed at any irradiation condition in the preliminary examination. After irradiation at 500°C, evidence of significant solute segregation was observed at grain boundaries and discrete precipitates were observed; precipitation was not observed in the room temperature irradiated samples. The grain boundary precipitates were highly enriched in Cr and Mn. Overall, the behavior of the high entropy alloy following irradiation at 500°C appears to be significantly different from the behavior observed in irradiated Fe-Cr-Ni austenitic alloys.

PROGRESS

Introduction

High entropy alloys introduced by Yeh *et al*. in 1995 [1-4] have changed the conventional alloy design in which only one or two principle elements decides the material primary properties. High entropy alloys (HEAs) are composed of four or more metallic elements mixed in an equimolar or near equimolar ratio. HEAs are specifically designed to form ductile solid-solution structures like face centered cubic (FCC) or body centered cubic (BCC) or mixtures of the two, instead of brittle intermetallic compounds. In recent years, HEAs have attracted significant attention due to their high strength, ductility, wear resistance, high temperature softening resistance and corrosion resistance, making them potential candidates for high temperature fusion structural applications. However, there is practically nothing known about their neutron radiation resistance. It is hypothesized that the high configurational entropy might promote enhanced point defect recombination in irradiated materials; the key objective of the present study is to examine the extent of microstructural and mechanical property changes produced by irradiation, compared to standard Fe-Cr-Ni FCC alloys.

Experimental

A high entropy alloy of composition 27%Fe-27%Mn-28%Ni-18%Cr, manufactured at ORNL, has been chosen for the present study. The material was prepared by arc melting by mixing

constituent metals of high purity. In general, the high entropy alloy should consist of approximately equimolar compositions in order to maximize configurational entropy. However, exploratory studies determined that the Fe-25%Mn-25%Ni-25%Cr alloy was not a single phase. Reducing the Cr composition resulted in a single FCC phase for an alloy composition of 27%Fe-27%Mn-28%Ni-18%Cr high entropy alloy.

The cast bar was homogenized at 1200 °C for 48 h, cold rolled and recrystallized at 900°C for 4hr in a vacuum furnace to obtain fully recrystallized microstructure with grain size of ~35µm. The neutron and ion irradiation experiments have been divided into two phases (Table 1). The first phase work covers the low temperature irradiation regime. The ion irradiations with 3 MeV Ni ions to fluences of 4.2 x 10^{13}, 4.2 x 10^{14} and 4.2 x 10^{15} ions/cm^2 (0.1, 1.0 and 10 dpa at a depth of 1.07 mm) were performed at room temperature and high temperature in the newly commissioned ORNL/University of Tennessee ion beam laboratory. The damage and implanted profile generated using SRIM [5] for 3 MeV Ni ions is shown in Fig-1. The Phase-I neutron irradiations to 0.1 and 1 dpa utilized perforated rabbit capsules in direct contact with the HFIR coolant water and were completed during the May fuel cycle. Rabbit capsule design work has been initiated for the Phase II (high temperature, 500°C) HFIR neutron irradiations, and the irradiations are expected to begin in late fall, 2013.

Table 1. Summary of completed (phase I) and planned/ in progress (phase II) neutron and ion irradiation conditions for the high entropy alloy.

Material		Ion irradiation (mid-range dose, ~3 MeV Ni ions)	HFIR neutron irradiation
HEA (Fe-28%Ni-27%Mn-18%Cr)	**Phase I**	0.1 dpa, room temp.	0.1 dpa, 70°C (perf. rabbit)
		1 dpa, room temp.	1 dpa, 70°C (perf. rabbit)
	Phase II	1 dpa, 500°C	1 dpa 500 ^{o}C
		10 dpa, 500°C	

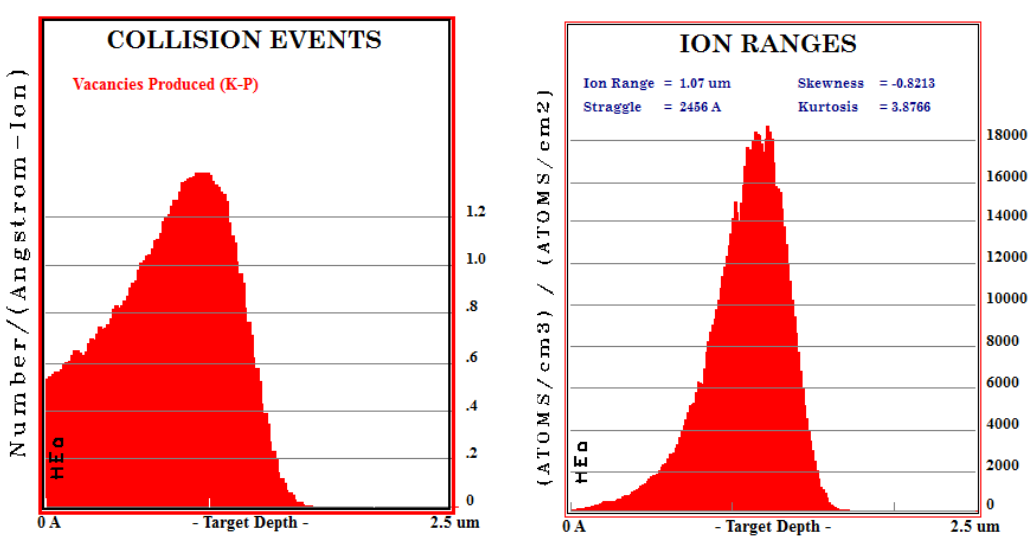

Fig 1. SRIM plots comparing the damage profile with the implanted Ni-atom profile.

Hardness measurements were performed at room temperature using a MTS XP nanoindenter. A Berkovich diamond indenter (3-sided pyramidal tip) was used for the tests. All the tests were performed in continuous stiffness measurement mode with a constant loading rate $\dot{P}/_{P} = 0.05\text{s}^{-1}$ and the maximum load applied is 150 mN [6]. For good statistical analysis, each sample was indented with at least 16 to 25 indents and the average of the results was used in the analysis. PANalytical Xpert diffractometer with $Mo_{K\alpha}$ (λ= 0.709319 A°) target was used to perform grazing incidence X-ray measurements (incidence beam fixed at 2°) on the ion-irradiated samples. All scans used 2mm adjustable slits and 2° anti-scatter slit so that the same portion of the sample was always in the X-ray beam throughout the scan. The detectable phase limit of the diffractometer is ≈3 wt.%, which means, any phase with less than 3 wt.% cannot be detected using this method.

Analysis of grain boundary composition of irradiated samples was performed using a scanning transmission microscope with energy diffraction spectrometry (STEM/EDS). STEM/EDS measurements was performed in a Philips CM200/FEG STEM which produces a probe of 1.4 nm at 200 KV operating voltage.

Preliminary Results and Discussion

Fig 2 shows the optical microstructure of the control sample after final heat treatment. The control HEA sample is etched with H_2O_2: HCl: H_2O (vol.% of 1:1:6) to obtain a better contrast of grain boundary. A single-phase polycrystalline structure was observed without any second phase. In addition, the ion-irradiated samples were investigated for potential phase and structural changes using XRD measurements. Interestingly, no detectable phase (> 3wt %) was observed as a function of irradiation temperature and dose rate (see Fig 3). Even at higher dose rates and temperatures, the HEAs are stable without forming any detectable second phase.

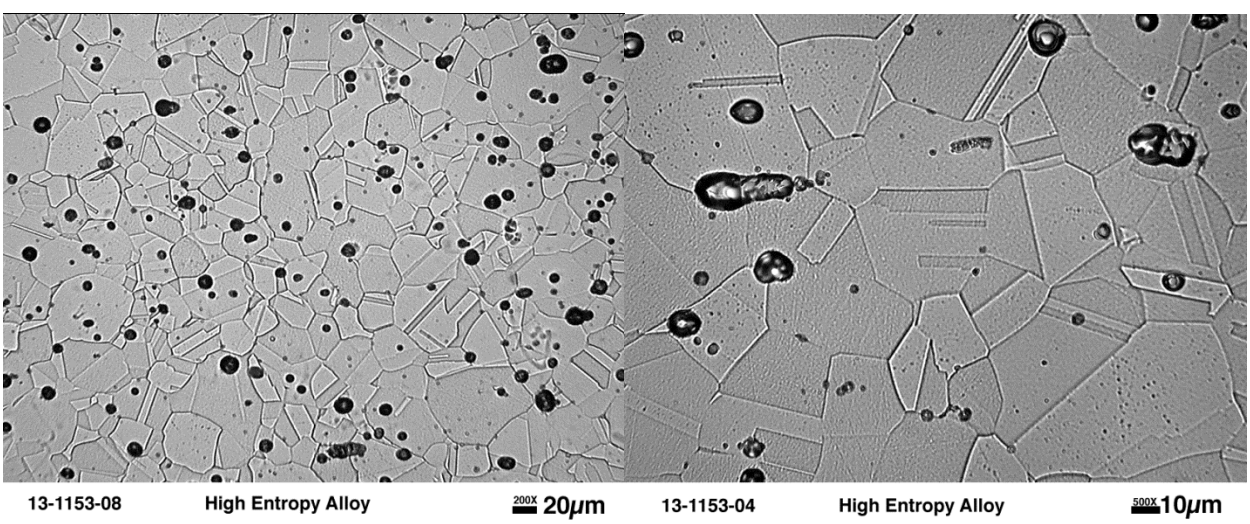

Fig 2. Optical micrographs of HEA control sample (Note: the black spots in the images are etch pits).

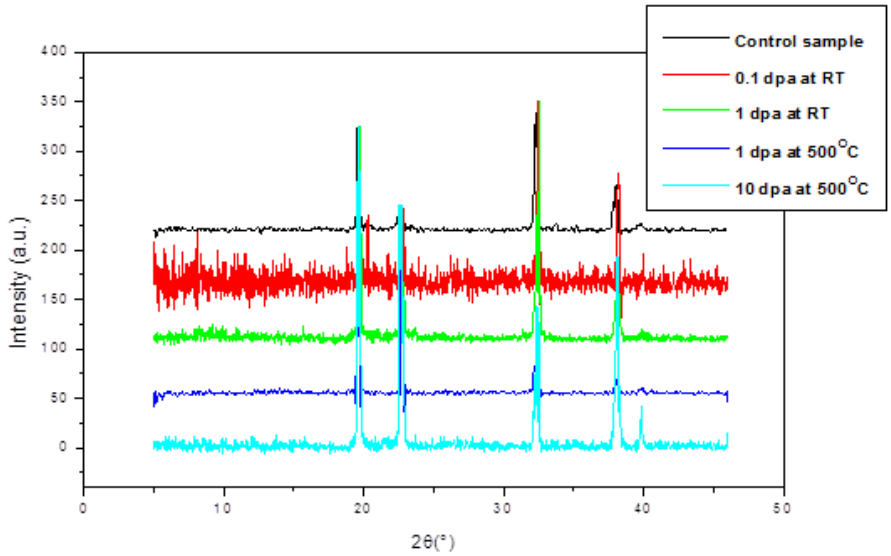

Fig 3. XRD patterns of the HEAs under different conditions.

Microstructure and Radiation Induced Segregation (RIS)

Void swelling in Fe-Ni-Cr alloys has a significant impact on its performance in the reactor [7-13]. Earlier studies have concluded that overall swelling of these alloys can be varied by varying Ni and Cr concentration [8,13]. In addition, ferritic steels showed more resistance to void swelling than austenitic steels [10]. In contrast to conventional Fe-Ni-Cr alloys, present HEA showed no pronounced void swelling for any irradiation conditions. Initial microstructural characterization focused on solute segregation and precipitation. Radiation induced segregation is a phenomenon in which the local alloy composition is altered by spatial redistribution of alloying element at the point defect sinks. This leads to enrichment or depletion of solute elements in defect sinks such as grain boundaries, phase boundaries, dislocations and voids.

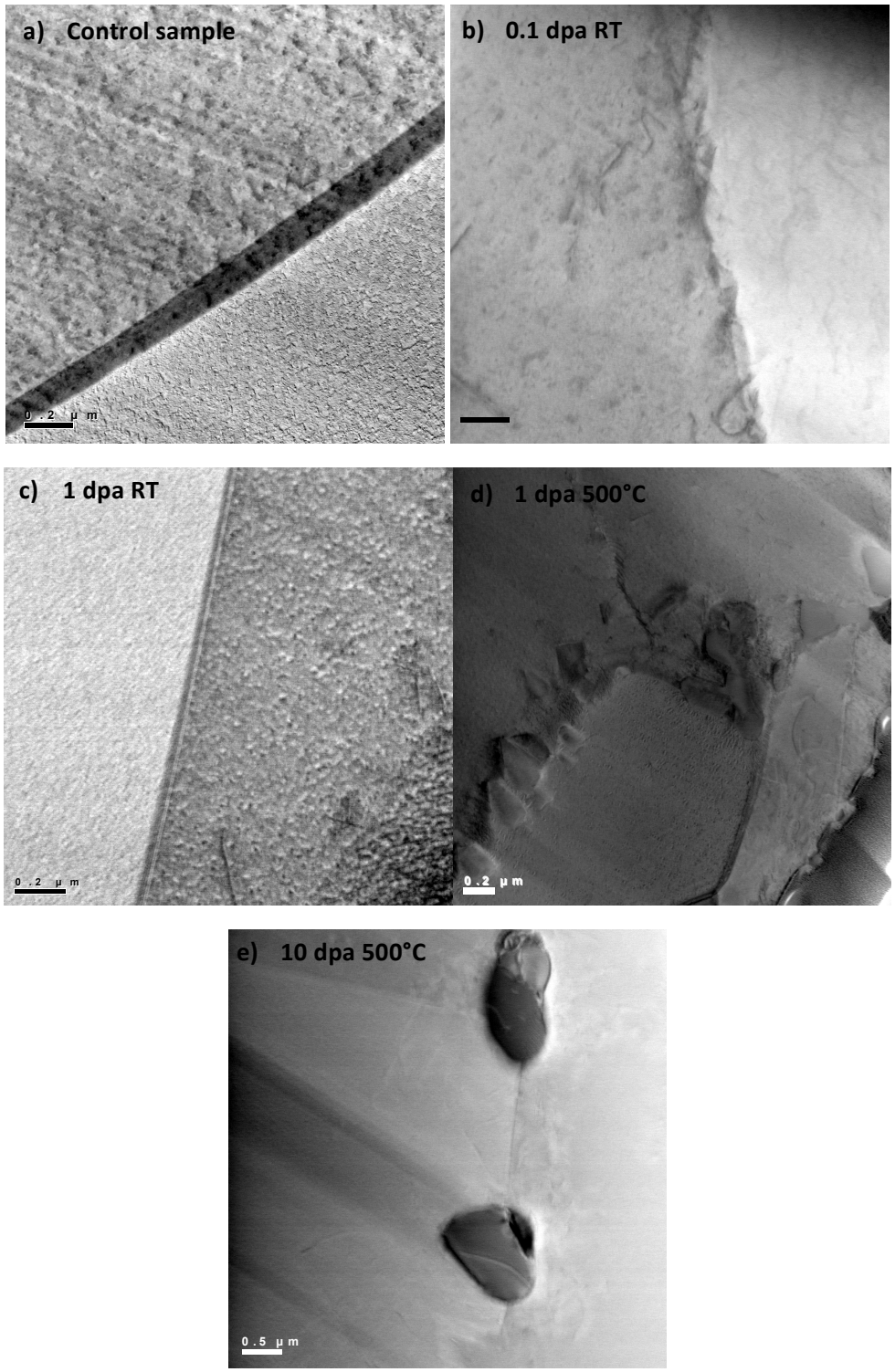

Fig 4. STEM micrographs of a) Control sample b) 0.1 dpa RT c) 1dpa RT d) 1 dpa 500°C sample d) 10 dpa 500°C (Note: detectable segregation at the grain boundary can be seen in 1 and 10 dpa, 500°C samples).

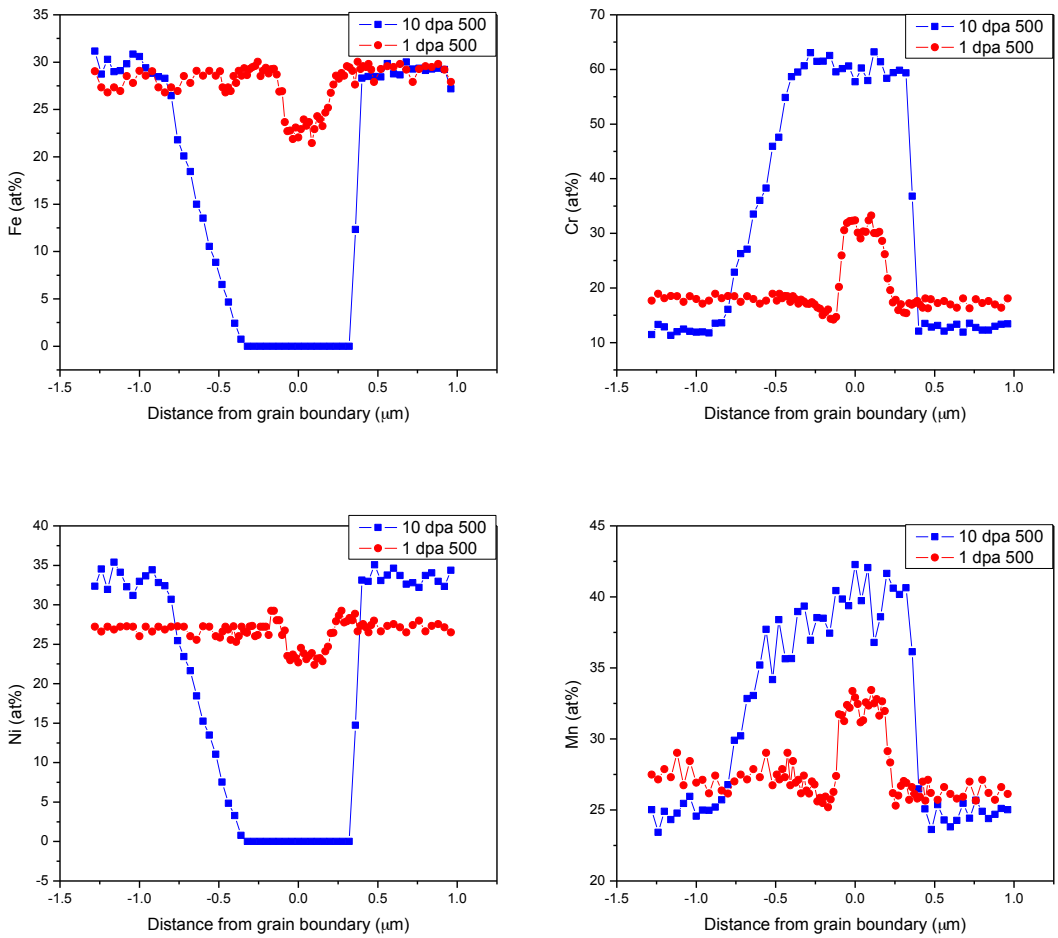

Fig-5. STEM/EDS grain boundary composition profiles of 1 dpa and 10 dpa samples irradiated at 500°C.

Fig 4 shows the STEM micrographs of the samples exposed to different irradiation conditions. As it can be seen in the micrographs, pronounced segregation (resulting in precipitation) was observed at the grain boundaries of the samples irradiated to 1 and 10 dpa at 500°C. Samples irradiated to 0.1 and 1 dpa at the room temperature showed no measurable segregation detectable by STEM/EDS. The same technique was performed across the grain boundary precipitates of the 1 and 10 dpa 500°C samples, to identify and quantify the compositions of those precipitates. Fig 5 shows the experimentally observed radiation induced segregation (RIS) of the samples that were ion irradiated to a dose of 1 and 10 dpa at 500°C. The segregation profile observed for Fe-Ni-Mn-Cr HEA (see Fig 5) is not a typical trend expected in Fe or Ni based or Fe-Ni-Cr alloys [14-16]. However, the complete understanding of RIS behavior of these alloys is still lacking. RIS typically causes depletion of fast diffusing elements like Cr. In contrast, enrichment of Cr at the grain boundaries is also reported in the literature for some ferritic alloys [17-21]. Recent studies have concluded that factors like alloying composition and temperature may determine the enrichment or depletion of an element [17]. In

the present HEA samples, Cr and Mn enrichment and Fe and Ni depletion was observed during ion irradiation at 500°C. In addition, as the radiation dose increases, the chromium and manganese becomes more enriched and the iron and nickel become progressively more depleted along the grain boundary. In general, it was shown in previous irradiation studies on conventional austenitic alloys that relatively slow diffusing Ni and Fe segregate to the defect sinks, while faster diffusing Cr and Mn atoms diffuse away from the defect sinks. The completely opposite behavior in the present FCC high entropy alloy compared to conventional Fe-Cr-Ni or Fe-Cr-Mn austenitic alloys could be due to some change in diffusion kinetics in HEAs or some other physical phenomenon. Unlike conventional alloys, in HEAs there is no solvent element that dominates the composition of the solid solution. In any case, the significant difference in radiation response for the HEA vs. conventional Fe-Cr-Ni-Mn alloys at 500°C is remarkable.

Hardness

Nanohardness is a key performance index for ion-irradiated samples. The normalized hardness values of irradiated samples are shown in Fig 6. The sample irradiated to 1 dpa at room temperature showed high hardness when compared with other irradiated samples. The increase in hardness with the increase in irradiation dose at room temperature can be due to the presence of strained regions formed by dislocation loops. In addition, it is more interesting to see that the hardness of samples irradiated to 1 and 10 dpa at 500°C is low and also very close to the hardness of control sample. Many hypothetical assumptions can be made from the present hardness results. However, one can get a clear understanding of the plot only after analyzing the irradiation defects using TEM, which will be performed in the next reporting period.

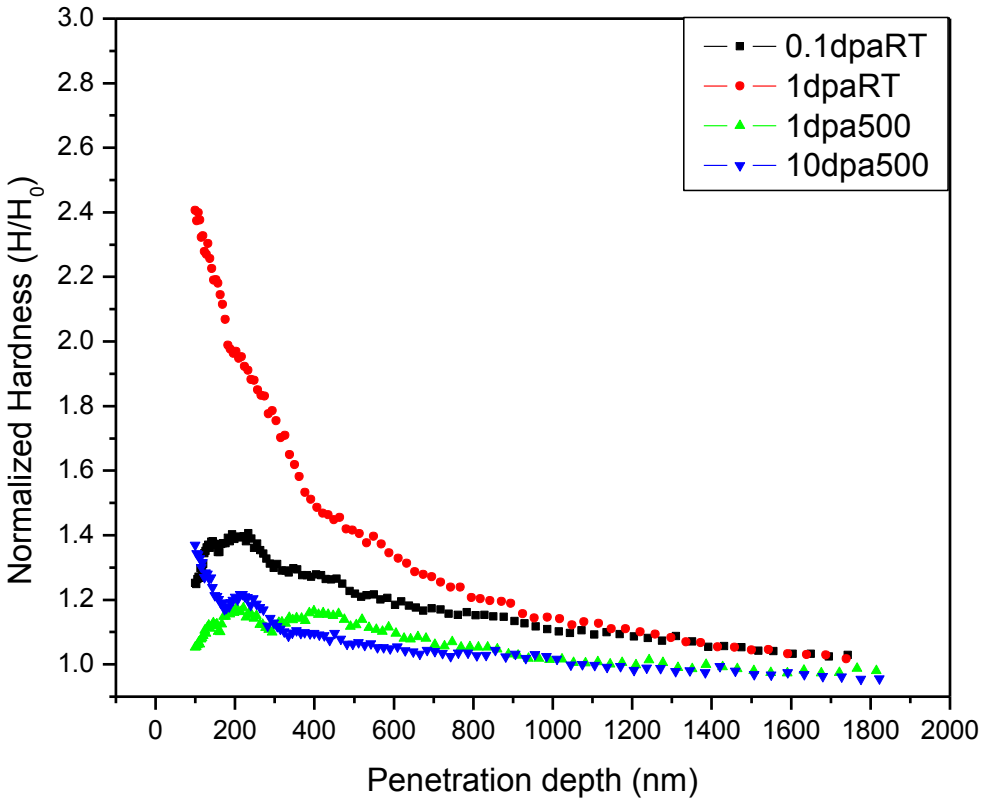

Fig 6. Nanoindentation normalized hardness plots.

FUTURE WORK

Quantitative TEM examination of ion-irradiated HEAs is ongoing. The comparison of radiation defects in irradiated samples with unirradiated control sample will be used to elucidate the self-healing through point defect recombination in HEAs. Phase-I neutron irradiation work on HEAs is complete and will undergo capsule disassembly in next few weeks. A variety of post-irradiation tests including TEM examination will be performed on the neutron irradiated samples. The capsule design for Phase II (500°C) neutron irradiations is in progress.

REFERENCES

[1] J. W. Yeh, S. K. Chen, S. Lin, J. Y. Gan, T. S. Chin, T. Shunt, C. H. Tsau, and S. Y. Chang, *Adv. Eng. Mater.* **6** (2004) 299.
[2] K. H. Huang and J. W. Yeh, Master's Thesis, National Tsing Hua University, (1996).
[3] C. Y. Hsu, J. W. Yeh, S. K. Chen, and T. T. Shun, *Metall. Mater. Trans. A* **35** (2004) 1465.
[4] J. W. Yeh, *Ann. Chim. Sci. Mater.* **3** (2006) 633.
[5] J. F. Ziegler, SRIM Software, Retrieved 1 July 2013, from http://www.srim.org/.
[6] W. C. Oliver and G. M. Pharr, *J. Mater. Res.* **7** (1992) 1564.

[7] S. J. Zinkle and G. S. Was, *Act. Mater*. **61** (2013) 735.
[8] F. S. James, *J. Nucl. Mater.* **141** (1986) 748.
[9] L. Marlies and M. Lorenzo, *Acta. Mater*. **59** (2011) 6547.
[10] H. K. D. H. Bhadeshia, *Mater. Sci. Eng. A* (1997) 64.
[11] F. A. Garner, M. B. Toloczko, and B. H. Sencer, *J. Nucl. Mater.* ***276*** (2000) 123.
[12] E. A. Little, D. A. Stow, *J. Nucl. Mater.* ***87*** (1979) 25.
[13] S. Ohnuki, F. A. Garner, and H. Takahashi, *Mater. Trans JIM* **34** (1993), 1031.
[14] G. S. Was, J. P. Wharry, B. Frisbie, B. D. Wirth, D. Morgan, J. D. Tucker, T. R. Allen, *J. Nucl. Mater.* **411** (2011) 41.
[15] T. R. Allen, J. T. Busby, J. Gan, E. A. Kenik, and G. S. Was, *ASTM STP* **1366** (2000) 739.
[16] S. J. Zinkle, P. J. Maziasz, and R. E. Stoller, *J. Nucl. Mater.* **206** (1993) 266.
[17] G. Gupta, Z. Jiao, A. N. Ham, J. T. Busby, and G. S. Was, *J. Nucl. Mater.* **351** (2006) 162.
[18] R. E. Clausing, L. Heatherly, R. G. Faulkner, A. F. Rowcliffe, and K. Farrell, *J. Nucl. Mater.* **141** (1986) 978.
[19] Z. Lu, R. G. Faulkner, N. Sakaguchi, H. Kinoshita, H. Takahashi, and P. E. J. Flewitt, *J. Nucl. Mater.* **351** (2006) 155.
[20] S. Ohnuki, H. Takahashi, and T. Takeyama, *J. Nucl. Mater*. **103** (1982) 1121.
[21] H. Takahashi, S. Ohnuki, T. Takeyama, and H. Kayano, *J. Nucl. Mater.* **96** (1981) 233.